Static In-wheel Wireless Charging Systems for Electric Vehicles

Chirag Panchal, Junwei Lu, Sascha Stegen

Abstract: Wireless charging is a popular upcoming technology with uses ranging from mobile phone charging through to electric vehicle (EV) charging. Large air gaps found in current EV wireless charging systems (WCS) pose a hurdle of its success. Air gaps in WCS cause issues in regards to efficiency, power transfer and electromagnetic compatibility (EMC) leakage issues. A static In-Wheel WCS (IW-WCS) is presented which significantly reduces the issues associated with large air gaps. A small scale laboratory prototype; utilizing a standard 10mm steel reinforced tyre, has been created and compared to a typical 30mm air gap. The IW-WCS has been investigated by experimental and finite element method (FEM) based electro-magnetic field simulation methods to validate performance.

Index Terms: Battery Electric Vehicles, Electromagnetic compatibility, Finite Element Method, Resonant Inductive Power Transfer, Static In Wheel Wireless Charging Systems, Wireless Charging systems, Wireless Power Transfer.

1 Introduction

WCS have been proposed as a way of permitting battery electric vehicles (BEVs) to charge without a physical connection to the distribution grid [1]. Even though there are many benefits to using WCS, methods of stationary WCS have still been restricted by three major obstacles: lack of in vehicle receiver location standards, large airgaps and misalignment of coils [2],[3]. The Society of Automotive Engineers (SAE) International and International electro technical commission (IEC) have been working on wireless power transfer (WPT) standards[4],[5]. Current WCS are limited to an airgap distance between the primary and secondary coils minimum of 150mm up to 300mm due to minimum legislated ground clearance of vehicles. Such airgap distance can result in typical coupling coefficient (k) ranging from 0.01 to 0.2 [2],[6],[7]. Larger airgap distance can lead to lower efficiency and power transfer performance due to poor coupling coefficient (k)[8]. Health and Safety also becomes a predominant issue with larger airgaps due to the potential for electromagnetic radiation leakage from the charging coils [9] as well with the case of coil misalignment. To improve the poor coupling coefficient, authors of [10],[11] suggested the use of a vehicle tyre, specifically the in-built steel belt (IBSB) as a capacitive receiver or as a radio frequency (RF) displacement current receiver. The use of an IBSB receiver; capacitive or RF displacement, can increase the coupling co-efficient over under body receivers but both technologies require different infrastructure over inductively coupled WCS.

- *Chirag Panchal is currently pursuing Doctor of philosophy degree in electrical and electronics engineering in Griffith University, Brisbane, Australia, PH-+61737353752. E-mail: C.panchal@griffith.edu.au*
- *Junwei Lu is a foundation professor at the Griffith School of Engineering in electric power engineering, Brisbane Australia, PH-+61737327596. E-mail: J.Lu@griffith.edu.au*
- *Sascha Stegen has been working as a Lecturer at the Griffith School of Engineering for electronic and energy, Brisbane, Australia, PH-+61737354397. E-mail: S.stegen@griffith.edu.au*

This incompatibility with inductively coupled charging makes it a difficult system to adopt. The proposed IW-WCS improves the coupling over traditional underbody WCS but does not have the same drawbacks of the capacitive or RF IBSB systems.2 Concept Development Of Static Iw-Wcs

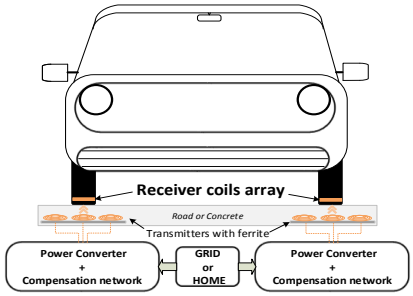

Fig 1. *Basic arrangement of a Static In-Wheel WCS*

Static inductance based IW-WCS have significant potential to integrate into the exiting stationary wireless electric vehicle charging system with additional advantages lower airgaps and higher coupling co-efficient between the primary and secondary sides. The basic arrangement of the fundamental design is presented in Fig.1.

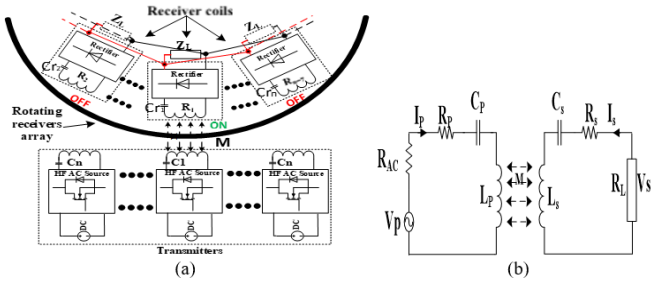

Fig. 2*. Series-series resonant In-Wheel WCS (a) schematic (b) the equivalent circuit*

In static IW-WCS, the transmitting coils are mounted under the road or beneath parking spots. These are connected to a high frequency (HF) AC source. The load; typically a battery is supplied through a rectifier and filter circuit inside the wheel and vehicle body. Unlike current WCS, the receiver coils including power converter and filtering circuitry are installed inside a tyre

in a parallel configuration as presented in Fig.2 (a). Series compensation topology has been employed in both sides of transmitter and receiver coils arrangement as it offers significant advantages such as the value of the capacitor in the source and receiver sides is independent from the load conditions and mutual inductance [12]. As the tyre is always in contact with the road surface, there is a major reduction in the airgap an increase in coupling coefficient and mutual inductance [13]. Fig. 2(b) illustrates the equivalent circuit of static IW-WCS, where L_p and L_s are the self-inductances of the primary and secondary windings and R_p and R_s are parasitic resistances of the windings, respectively. C_p and C_s are the series resonant capacitances for the both winnings in order to resonant the circuit. R_L is the load resistance at the receiver side of WCS. The input voltage of the WSC can be defined via:

$$\begin{bmatrix} V_p \\ 0 \end{bmatrix} = \begin{bmatrix} R_{AC} + R_p + j(\omega L_p - \frac{1}{\omega C_p}) & -j\omega M \\ -j\omega M & R_L + R_s + j(\omega L_s - \frac{1}{\omega C_s}) \end{bmatrix} \begin{bmatrix} I_p \\ I_s \end{bmatrix} \quad (1)$$

In order to determine the primary (Z_p) and secondary (Z_s) impedances of the wireless transformer equation (2) is em ployed.

$$Z_p = R_{AC} + R_p + j\left(\omega L_p - \frac{1}{\omega C_p}\right) \&$$

$$Z_s = R_s + R_L + j\left(\omega L_s - \frac{1}{\omega C_s}\right) \quad (2)$$

Consequently, equation (3) can be rewritten for primary (I_p) and secondary (I_s) currents by substitute (2) into (1).

$$\begin{bmatrix} I_p \\ I_s \end{bmatrix} = \frac{1}{Z_p \cdot Z_s + (\omega M)^2} \begin{bmatrix} Z_s & -j\omega M \\ -j\omega M & Z_p \end{bmatrix} \begin{bmatrix} V_p \\ 0 \end{bmatrix} \quad (3)$$

The power transfer efficiency (η) is the ratio of the output power and input power including losses as shown in (4).

$$\eta = \frac{P_{out}}{P_{in} + P_{Loss}} = \frac{(\omega M)^2 \times R_L}{|Z_s[Z_p \cdot Z_s + (\omega M)^2]| cos\varphi} \quad (4)$$

Apart from the switching and airgap losses, the system suffers from additional losses due to leakage inductance by the IBSB into the tyre, depending on the mutual inductance and attached load over the primary and secondary sides impedances. The maximum power transfer depends on several factors such as tyre size, possible wire cross section of the receiving as well as transmitting coil, the possible voltage levels as well as frequency. The proposed wireless charging system can be utilized as an efficient substitute in order to increase the range of the vehicle if the existing wireless charging is suffering from the airgap losses and poor coupling co-efficient. In addition, the absent of the ferrite core material on the secondary side also decreases the weight of the vehicle. However, it increases flux leakage on the receiving side due to the lack of the magnetic ferrite. As a result, it affects the overall power transfer efficiency.

3 System Design of Static IW-WCS

3.1 Structure arrangement

A detailed structural arrangement of the proposed IW-WCS is displayed in Fig. 3. The receiving coils are mounted on the rubber surface inside the tyre due to manufacturing limitations. Furthermore Fig. 3(a) shows that the electrical power transport from the tyre to the battery charging circuit is utilized by slips-rings: positive and negatives on the tyre rim. In order to reduce copper resistance of the circular plates, both plates were designed optimized cross-sectional area with minimal total losses. Seven coils are utilized in parallel configuration but the number of receiver coils depends on the specifications of a tyre. A demonstration of the receiver coil placement is presented in Fig. 3 (b) where the height and width of the tyre is provided. The output of the receiver coils are connected in parallel configuration so only active receiver coils receives power from the transmitter. The steel or alloy rim can provide structural support as well as provide additional shielding from the transmitting coil. There are several layers encased in the rubber to ensure safe vehicle travel, and to provide protection against punctures and gashes. As shown in Fig. 3 (c), the layer containing the steel belt and body ply is the proposed future location for the IW-WCS receiving coil. Integration of litz receiving coils and converters into tyre rubber and exporting power from the tyre to the body of the vehicle are the next major obstacles to overcome to make the IW-WCS a major success.

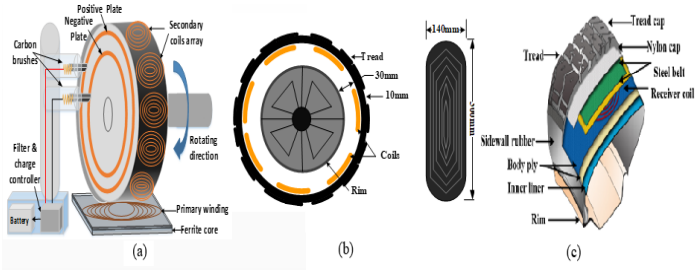

Fig. 3. *Structure arrangement of IW-WCS for EVs: (a) overview (b) coil arrangement and dimensions (c) future mounting location.*

3.2 Wireless Transformer Topology

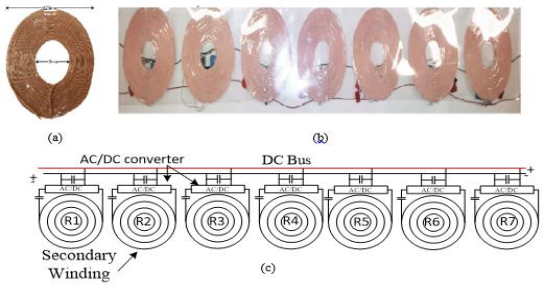

Fig 4. *Wireless transformer (a) primary (b) secondary coils array(c) connection diagram of secondary coil array*

Fig. 4 shows the primary coil and secondary coil array of the wireless transformer for the IW-WCS. The primary winding has been optimized for maximum mutual inductance in accordance to the secondary side size limitations. The dimensions and weights of the secondary coils are important, as incorrect de-

sign can lead to reduced tyre performance and unwanted magneto-friction. As shown in Fig. 4(b) and (c), the secondary coil array is created by connecting individual receiver coils in conjunction with a rectifier and filter circuit together in parallel to the DC bus. In this way, individual receiver coils operate independently as well as efficiently. The operational frequency for this WCS is 100 kHz. Both coils are wound with Litz wire to reduce Ohmic losses and increase coupling coefficient at HF. By utilizing litz wires the system has a higher Q value, therefore can increase maximum achievable efficiency due to the reduction of lower skin and proximity effects. The inner radius of the both windings is designed in a way that it provides a higher magnetic influence [13]. The WCS has a turn ratio of 1:1.87 to attain step up voltage in order to compensate the airgap losses. By introducing magnetic ferrite material, the inductance of the primary coil can be increased to 83 µH. Table 1 shows the specifications of the wireless transformer coils.

TABLE 1: *SPECIFICATIONS OF PRIMARY AND SECONDARY COILS*

Windings		Primary	Secondary
Number of turns (N)		23	43
Diameter (mm)	Inner/Outer	47/123	30/105
Cross-sectional area - copper (mm^2)		1.5	0.64
Inductance Without Ferrite (µH)	Calculated	50	122
	Simulated	49	124
	Measured	50	123
Quality factor (Q)@100kHz		150	107

4 Experimental set-up for Static IW-WCS

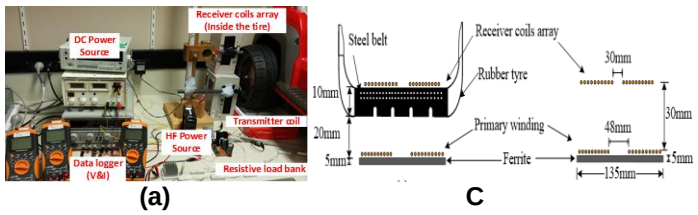

Fig. 5. (a) *Experimental arrangement set-up(b) 10mm thick IBSB rubber tyre plus 20mm airgap (c) 30mm air-gap with primary and secondary windings for static IW-WCS*

As shown in Fig. 5 (a), a small scaled experimental prototype was created to investigate wireless power transfer efficiency from source to receiver. To determine the performance effects of a tyre with an IBSB, its rubber thickness and airgap between two coils, two scenarios of the optimized distance [14] a 30mm airgap incorporating an IBSB tyre and 30mm airgap were investigated. A 30nF and 22nF capacitors were implemented at the primary and secondary sides to create series-series (SS) resonant at 100 kHz, respectively. For the experiment, the coils are perfectly aligned. The output power and efficiency were measured for load resistance 20 to 140Ω for two configurations,a 30mm airgap and 30mm airgap incorporating an ISBS tyre, as presented in Fig. 5(b)&(c).

5 Result and Analysis of Static IW-WCS

A small scaled experimental prototype of static IW-WCS has been examined by experimental and simulation methods to investigate the magnetic flux distribution, coupling co-efficient, power transfer efficiency and misalignment issue.

5.1 Magnetic field simulation results

In order to determine the magnetic flux distribution in the static IW-WCS and improving the system performance further, an axisymmetric model of the 10mm IBSB tyre with 20mm airgap setup, Fig. 5(b); was simulated at 100 kHz. As presented in Fig. 6, the magnetic permeability of a tyre is approximately 1 as it is similar to the permeability of air. The contour shows the magnetic flux distribution between two windings. The red spot at the edges of the primary winding presents the maximum magnetic flux density for the model. As the IBSB is made of conductive steel, some magnetic flux is absorbed. As a result, a slight increase in the leakage magnetic flux can be noted. The increased leakage inductance reduces the mutual inductance between two coils, as a result the simulated coupling coefficient reduces from 0.42 to 0.40 for the 10mm IBSB tyre plus 20mm airgap in the comparison to the 30mm airgap. By incorporating an aluminium rim 40mm away from the secondary winding (thickness of a tyre wall), the simulation shows a reduction in leakage inductance from 70 µH to 68 µH and an improved *k*. So the reduction of overall leakage magnetic flux can help to minimize the health and safety related issues associated with the WCS.

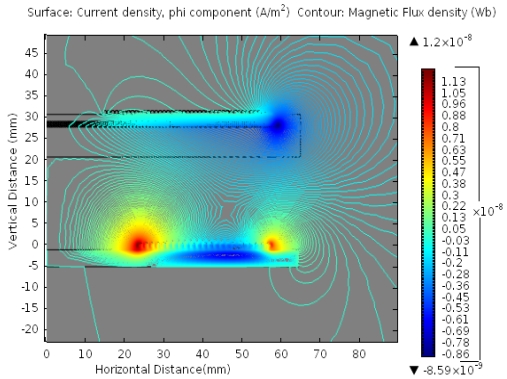

Fig. 6. *Simulation result of the 10mm IBSB tyre with 20mm airgap version*

5.2 Power and Efficiency results

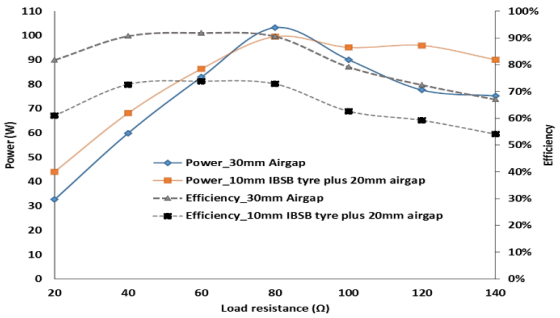

Fig. 7. *Power and Efficiency measurement of Static IW-WCS*

In order to analyse the effect of the ISBS of a standard tyre, power and efficiency measurements were taken and compared with that of just an airgap (Fig. Fig. 7). Without the wireless

transformer, the converter has an efficiency of ~85%. These results show that the maximum power transfer of the 10mm tyre with IBSB with a 20mm airgap configuration was 100W at 88 V whereas the 30mm airgap test has noted 103W at 90 V at 80Ω. The peak power transfer efficiency of the 30mm airgap was 92% between the ranges of 40Ω and 80Ω, with a gradual reduction in efficiency of 70% through to 140Ω. The 10mm IBSB tyre incorporating a 20mm airgap design follows the same trend but the efficiency drops around 18% through the range, with a maximum efficiency 74% from load resistances 40Ω to 80Ω. Overall, a 3% reduction in power and 18% efficiency drop are noted due to the IBSB in a tyre. This reduction in power transfer and efficiency can be attributed to eddy currents circulating through the IBSB.

5.3 Power Efficiency and Misalignment result

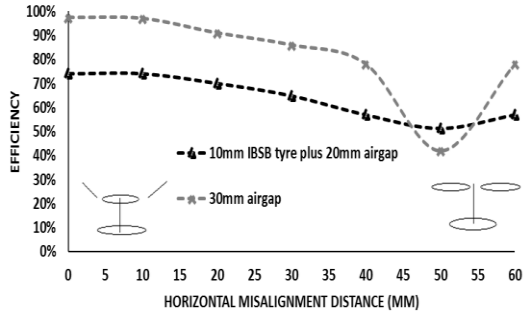

Fig. 8. *Power efficiency via horizontal misalignment distance*

As mentioned before alignment tolerance test is very crucial in the WPT in order to investigate the misalignment effect on coupling coefficient and power transfer efficiency When two coils are aligned perfectly, the coupling coefficient of the 10mm IBSB tyre plus 20mm airgap configuration (0.27) is slightly lower than the 30mm airgap version (0.33) due to the loss of magnetic flux at the inbuilt steel belt. Increasing the horizontal misalignment between the two coils has a significant negative effect on not only coupling coefficient but also on the power transfer efficiency. With a 50mm horizontal misalignment distance, the maximum power transfer reduced approximately by 35% resulting in a power of 65W and efficiency of 50%, as shown in Fig. 8. Two receiver coils from the array were aligned and activated with the transmitter coil simultaneously, which caused a reduction of flux density. As a result, drop power and thus efficiency occurs. When the X-direction horizontal displacement occurs beyond 50mm, the neighboring coil in the receiver coil array starts receiving power from the transmitter coil. As a result, the misalignment and consequently the power delivery problems in the static IW-WCS is resolved to some extent with the help of neighboring coil activation due to the parallel multi-receiver array structure. However, the power transfer efficiency significantly drops when a horizontal displacement in Y-direction arises, as there is no additional receiver coil in this direction.

6 Conclusion

A novel Static IW-WCS for EVs has been proposed in this paper in order to investigate the effect of IBSB based technology. A 10mm thick IBSB tyre based laboratory prototype was built and investigated. The same experiments are conducted with an equivalent air-gap to normalize the rubber tyre results. The developed design and principle experiments show that it is possible to transfer wireless power relatively efficiently in the 10mm thick rubber tyre plus 20mm airgap as well as 30mm airgap without IBSB. In addition, IW-WCS has higher power transfer capabilities in comparison with capacitive or RF IBSB Via-Wheel systems. FEM simulation method was utilized to analyse the magnetic flux and leakage flux distribution and to further proof that the proposed concept is efficient in regards to the flux distribution and eddy currents. Further investigations will be made regarding communication techniques and efficiency improvements through the implementation of large-scale prototypes.

References

[1] A. Kamineni, G. A. Covic, and J. T. Boys, "Analysis of Coplanar Intermediate Coil Structures in Inductive Power Transfer Systems," IEEE Transactions on Power Electronics, vol. 30, pp. 6141-6154, 2015.

[2] D. M. Vilathgamuwa and J. P. K. Sampath, "Wireless Power Transfer (WPT) for Electric Vehicles (EVs)—Present and Future Trends," in Plug In Electric Vehicles in Smart Grids, S. F. Rajakaruna S., Ghosh A., Ed., ed Springer International Publishing AG, Part of Springer Science+Business Media: Springer Singapore, 2015, pp. 33-60.

[3] S. Jaegue, S. Seungyong, K. Yangsu, A. Seungyoung, L. Seokhwan, J. Guho, et al., "Design and Implementation of Shaped Magnetic-Resonance-Based Wireless Power Transfer System for Roadway-Powered Moving Electric Vehicles," Industrial Electronics, IEEE Transactions on, vol. 61, pp. 1179-1192, 2014.

[4] "SAE International Approves TIR J2954 for PH/EV Wireless Charging," ed. Warrendale,Pennsylvania, United States: SAE INternational, 2016, p. 1.

[5] D. Leskarac, C. Panchal, S. Stegen, and J. Lu, "PEV Charging Technologies and V2G on Distributed Systems and Utility Interfaces," in Vehicle-to-Grid: Linking Electric Vehicles to the Smart Grid. vol. 79, J. Lu and J. Hossain, Eds., ed London, United Kingdom: The Institution of Engineering and Technology (IET), 2015, pp. 157-209.

[6] V. Jiwariyavej, T. Imura, and Y. Hori, "Coupling Coefficients Estimation of Wireless Power Transfer System via Magnetic Resonance Coupling Using Information From Either Side of the System," IEEE Journal of Emerging and Selected Topics in Power Electronics, vol. 3, pp. 191-200, 2015.

[7] X. Zhang, Z. Yuan, Q. Yang, Y. Li, J. Zhu, and Y. Li, "Coil Design and Efficiency Analysis for Dynamic Wireless Charging System for Electric Vehicles," IEEE Transactions on Magnetics, vol. 52, pp. 1-4, 2016.

[8] K. Kalwar, S. Mekhilef, M. Seyedmahmoudian, and B. Horan, "Coil Design for High Misalignment Tolerant Inductive Power Transfer System for EV Charging," Energies, vol. 9, p. 937, 2016.

[9] H. Jiang, P. Brazis, M. Tabaddor, and J. Bablo, "Safety considerations of wireless charger for electric vehicles — A review paper," in 2012 IEEE Symposium on Product Compliance Engineering (ISPCE), Portland, OR, 2012, pp. 1-6.

[10] T. Ohira, "Via-wheel power transfer to vehicles in motion," in Wireless Power Transfer (WPT), 2013 IEEE, 2013, pp. 242-246.

[11] Y. Suzuki, T. Sugiura, N. Sakai, M. Hanazawa, and T. Ohira, "Dielectric coupling from electrified roadway to steel-belt tires characterized for miniature model car running demonstration," in Microwave Workshop Series on Innovative Wireless Power Transmission: Technologies, Systems, and Applications (IMWS), 2012 IEEE MTT-S International, 2012, pp. 35-38.

[12] M. Chinthavali, W. Zhiqiang, and S. Campbell, "Analytical modeling of wireless power transfer (WPT) systems for electric vehicle application," in 2016 IEEE Transportation Electrification Conference and Expo (ITEC), 2016, pp. 1-8.

[13] R. Bosshard, J. Muhlethaler, J. W. Kolar, and I. Stevanovic, "Optimized magnetic design for inductive power transfer coils," in Applied Power Electronics Conference and Exposition (APEC), 2013 Twenty-Eighth Annual IEEE, 2013, pp. 1812-1819.
\

[14] C. Panchal, D. Leskarac, J. Lu, and S. Stegen, "Investigation of flux leakages and EMC problems in wireless charging systems for EV and other mobile applications," in Environmental Electromagnetics (CEEM), 2012 6th Asia-Pacific Conference on, 2012, pp. 301-304.